BRIEF ARTICLE

Sorafenib inhibits growth and metastasis of hepatocellular carcinoma by blocking STAT3

Fang-Ming Gu, Quan-Lin Li, Qiang Gao, Jia-Hao Jiang, Xiao-Yong Huang, Jin-Feng Pan, Jia Fan, Jian Zhou

Fang-Ming Gu, Quan-Lin Li, Qiang Gao, Jia-Hao Jiang, Xiao-Yong Huang, Jin-Feng Pan, Jia Fan, Jian Zhou, Liver Cancer Institute, Zhongshan Hospital and Shanghai Medical School, Fudan University, Shanghai 200032, China

Correspondence to: Jian Zhou, MD, PhD, Liver Cancer Institute, Zhongshan Hospital and Shanghai Medical School, Fudan University, 180 Feng Lin Road, Shanghai, 200032, China. zhou.jian@zs-hospital.sh.cn
Telephone: +86-21-64037181 Fax: +86-21-64037181

Abstract

AIM: To investigate the inhibitory role and the underlying mechanisms of sorafenib on signal transducer and activator of transcription 3 (STAT3) activity in hepatocellular carcinoma (HCC).

METHODS: Human and rat HCC cell lines were treated with sorafenib. Proliferation and STAT3 dephosphorylation were assessed. Potential molecular mechanisms of STAT3 pathway inhibition by sorafenib were evaluated. *In vivo* antitumor action and STAT3 inhibition were investigated in an immunocompetent orthotopic rat HCC model.

RESULTS: Sorafenib decreased STAT3 phosphorylation at the tyrosine and serine residues (Y705 and S727), but did not affect Janus kinase 2 (JAK2) and phosphatase shatterproof 2 (SHP2), which is associated with growth inhibition in HCC cells. Dephosphorylation of S727 was associated with attenuated extracellular signal-regulated kinase (ERK) phosphorylation, similar to the effects of a mitogen-activated protein kinase (MEK) inhibitor U0126, suggesting that sorafenib induced S727 dephosphorylation by inhibiting MEK/ERK signaling. Meanwhile, sorafenib could also inhibit Akt phosphorylation, and both the phosphatidylinositol-3-kinase (PI3K) inhibitor LY294002 and Akt knockdown resulted in Y705 dephosphorylation, indicating that Y705 dephosphorylation by sorafenib was mediated by inhibiting the PI3K/Akt pathway. Finally, in the rat HCC model, sorafenib significantly inhibited STAT3 activity, reducing tumor growth and metastasis.

CONCLUSION: Sorafenib inhibits growth and metastasis of HCC in part by blocking the MEK/ERK/STAT3 and PI3K/Akt/STAT3 signaling pathways, but independent of JAK2 and SHP2 activation.

Gu FM, Li QL, Gao Q, Jiang JH, Huang XY, Pan JF, Fan J, Zhou J. Sorafenib inhibits growth and metastasis of hepatocellular carcinoma by blocking STAT3. *World J Gastroenterol* 2011; 17(34): 3922-3932 Available from: URL: http://www.

INTRODUCTION

Hepatocellular carcinoma (HCC) is the fifth most common cancer and the third most frequent cause of cancer-related death globally. Although prognosis of patients with HCC has increased in recent decades, long-term survival remains unsatisfactory because of the high rate of recurrence and metastasis[1]. Advances in treating this disease are likely to develop from a better understanding of its biology and behavior, which are affected by multiple molecular pathways controlled by transcription factors[2,3].

Signal transducer and activator of transcription 3 (STAT3) plays a critical role in transcriptional regulation of genes that are involved in tumor cell proliferation, survival and invasion[4]. Constitutive activation of STAT3 is observed in 72.4% of human HCC[5] and in a wide variety of other cancer types[6,7]. Overexpression of constitutively activated forms of STAT3 induces the formation of foci *in vitro* and tumors in mouse models. Moreover, inhibiting STAT3 function *via* RNA knockdown, peptide inhibition, and expression of dominant-negative forms in cancer cells leads to a decrease in tumor progression[8]. Our group has also reported that knockdown of STAT3 with antisense oligonucleotides inhibits tumor growth and metastasis in a mouse xenograft model of HCC[9]. In human HCC tissues, constitutive activation of STAT3 is a significant predictor of overall survival[5]. Thus, targeting of STAT3 activation may prove to be an effective approach to controlling HCC.

Sorafenib (Nexavar, BAY 43-9006) is a multikinase inhibitor that has shown anti-tumor activity against a wide variety of cancers including HCC[10,11]. Sorafenib blocks tumor cell proliferation and angiogenesis by targeting the Raf/mitogen-activated protein kinase kinase (MEK)/extracellular signal-regulated kinase (ERK) signaling pathway and receptor tyrosine kinases (RTKs), such as vascular endothelial cell growth factor receptor (VEGFR)-2, VEGFR-3, platelet-derived growth factor receptor-β, fms-like tyrosine kinase receptor-3 (FLT3), RET, and c-KIT[10,11]. Recently, sorafenib has been shown to suppress tumor growth by decreasing STAT3 phosphorylation in a group of human malignancies[12-15]. In HCC, sorafenib has also been suggested to overcome TRAIL resistance through the inhibition of STAT3[16]. However, thus far, the exact molecular mechanisms by which sorafenib inhibited STAT3 have not been fully elucidated.

Here, we found that sorafenib decreased STAT3 phosphorylation at both tyrosine and serine residues (Y705 and S727), which were independent of Janus kinase 2 (JAK2) and phosphatase shatterproof 2 (SHP2) activity. We further demonstrated that inhibition of the phosphatidylinositol-3-kinase (PI3K)/Akt and MEK/ERK pathways was responsible for Y705 and S727 dephosphorylation, respectively, by sorafenib. Consistent with these findings, sorafenib markedly inhibited STAT3 dephosphorylation, suppressed tumor growth and metastasis in an immunocompetent orthotopic rat HCC model.

MATERIALS AND METHODS

Reagents and cell lines

Sorafenib (BAY 43-9006, Bayer Pharmaceutical Corporation) was dissolved in sterile dimethyl sulfoxide (DMSO) for *in vitro* experiments, and in Cremophor EL (Sigma) and 95% ethanol (50:50) for *in vivo* experiments. DMSO was added to cultures at 0.1% (v/v) final concentration as a vehicle control. Primary antibodies, STAT3 and phosphorylated STAT3 (p-STAT3; Y705 and S727); Akt and phosphorylated Akt (p-Akt; S473); JAK2 and phosphorylated JAK2 (p-JAK2; Y1007/1008); ERK1/2 and phosphorylated ERK1/2 (p-ERK1/2; T202/Y204); SHP2 and phosphorylated SHP2 (p-SHP2; Y580) were purchased from Cell Signaling Technology. Cyclin D1 was from Abcam. Glyceraldehyde-3-phosphate dehydrogenase (GAPDH) was purchased from Millipore. Human or rat Akt small interfering RNA (siRNA), control siRNA, were obtained from Shanghai GenePharma Co. (Shanghai, PR China). LY294002, a PI3K inhibitor, and U0126, a MEK inhibitor, were purchased from Cell Signaling Technology.

Two human HCC cell lines, HCCLM3[17,18] and HepG2 (ATCC), and a rat HCC cell line, Morris hepatoma 3924A (MH) cells (German Cancer Research Center Tumor Collection)[19], were maintained in high-glucose DMEM supplemented with 10% heat-inactivated fetal bovine serum, L-glutamine, 100 units/mL penicillin, and 100 μg/mL streptomycin. Cell lines were cultured at 37 ℃ in a humidified incubator in 5% CO_2.

MTT assay

The effect of sorafenib on HCC cell growth was determined with the 3-[4,5-dimethylthiazol-2-yl]-2,5-diphenyltetrazoliumbromide (MTT) assay. Cells were seeded into 96-well flat-bottom plates (1×10^3/well) and cultured for 24, 48 or 72 h in medium supplemented with sorafenib (0, 0.05, 0.1, 1, 5, 10 or 20 μmol/L; 6 wells/dose), and each experiment was repeated at least three times. After sorafenib treatment, cells were incubated with MTT (20 μL/well) at 37 ℃ for 4 h, and then 200 μL DMSO was added. The absorbance of individual wells was determined at 570 nm.

Western blotting analysis

Western blot analysis was performed as previously described[20]. Briefly, total cell lysates were prepared, and proteins were separated by SDS-PAGE, followed by transfer to polyvinylidene difluoride membranes. The membranes were washed, blocked, and incubated with the specific primary antihuman antibodies against p-STAT3-Y705 (1:1000), p-STAT3-S727 (1:1000), STAT3

(1:1000), p-Akt (1:1000), Akt (1:1000), p-ERK1/2 (1:1000), ERK1/2 (1:1000), p-JAK2 (1:1000), JAK2 (1:1000), p-SHP2 (1:1000), SHP2 (1:1000), cyclin D1 (1:1000), or GAPDH (1:5000), followed by incubation with horseradish peroxidase-conjugated secondary antibodies. Proteins were detected by enhanced chemiluminescence assay (Pierce-Thermo Scientific).

Quantitative reverse transcription-polymerase chain reaction

Cells were plated and treated with 10 μmol/L sorafenib. The cells were harvested after 24 h, and total RNA was extracted with Trizol Reagent (Invitrogen) according to the manufacturer's protocol. Total RNA was reverse transcribed with RevertAid™ first-strand cDNA synthesis kit (Fermentas). Human and rat STAT3 mRNA levels were determined by qPCR using SYBR Premix Ex Taq (Ta-KaRa, Dalian, China) and normalized to human and ratβ-actin respectively, using the following primers: β-actin (human) forward, 5'-CAA CTG GGA CGA CAT GGA GAA AAT-3' and reverse, 5'-CCA GAG GCG TAC AGG GAT AGC AC-3'; β-actin (rat) forward, 5'-TCC ACC CGC GAG TAC AAC CTT CTT-3' and reverse, 5'-GGC CCG GGG AGC ATC GTC-3'; STAT3 (human) forward, 5'-CCC CCG CAC TTT AGA TTC AT-3' and 5'-GGT AGG CGC CTC AGT CGT AT-3'; STAT3 (rat) forward, 5'-GGT GAT GAG TTT CCG AGT GTG TCT GA-3' and reverse, 5'-AAA GCG CCT GCG CCT GCG ATA AAG TTC T-3'. Relative gene expression was calculated with the $2^{-\Delta Ct}$ method.

Akt silencing by siRNA

Akt siRNA and negative control mismatch sequences were transfected into HepG2 and MH cells using Lipofectamine™ 2000 (Invitrogen) according to the manufacturer's instructions. The following sense and anti-sense siRNA strands were used: Akt (human) GUG CCA UGA UCU GUA UUU ATT (sense), UAA AUA CAG AUC AUG GCA CTT (anti-sense); Akt (rat) GCU CAG AUG AUC ACC AUC ATT (sense), UGA UGG UGA UCA UCU GAG CTT (anti-sense). After 72 h, cells were lysed, and protein was analyzed by Western blotting.

Animal experiments

Male ACI rats (Harlan Inc., Indianapolis, IN, United States; 200-220 g) were maintained in laminar-flow cabinets under specific pathogen-free conditions and a 12-h dark-light cycle. The animals were cared for and handled according to recommendations of the NIH guidelines for care and use of laboratory animals. The Shanghai Medical Experimental Animal Care Committee approved the experimental protocol. Intrahepatic tumor implantation with Morris Hepatoma fragments was performed under aseptic conditions as previously described[21].

The rats were randomly assigned to 3 groups (*n* = 10 per group): vehicle control, sorafenib early treatment, and sorafenib late treatment. Sorafenib treatment groups were given 30 mg/kg sorafenib in 500 μL carrier solu-

tion once daily by gavage. The dose of sorafenib was based on doses commonly used in murine models[11,22]. Treatment was started on days 5 and 17 after tumor implantation in the sorafenib early and late treatment groups, respectively. On day 17, the HCC xenografts reached approximately 700 mm³, which was demonstrated in our preliminary experiment. Control rats received an equal volume of carrier solution by gavage. The rats were sacrificed at day 38 after tumor implantation. At necropsy, tumor volume was calculated as V =π/6 × length × width × height. Lung and lymph node metastasis, as well as peritoneal seeding, were denoted as the visually positive tumor nodules. For Western blot analysis, tumor tissues were homogenized in tumor lysis buffer. For immunohistochemical staining, tumors were fixed in paraformaldehyde for 24 h and embedded in paraffin for sectioning.

Immunohistochemistry

Tissue sections (4 μm) were stained with hematoxylin and eosin for histologic analysis and with the specific primary antihuman antibodies against p-STAT3-Y705, p-STAT3-S727, p-Akt, p-ERK and cyclin D1 for immunohistochemistry. Briefly, after microwave antigen retrieval, tissues were incubated with primary antibodies overnight at 4 ℃, followed by 30-min incubation with the secondary antibody. The reaction was visualized with diaminobenzidine, and tissues were counterstained with hematoxylin.

The tissue sections were viewed at × 200 magnification and images were captured. Five fields per section were analyzed, excluding peripheral connective tissue and necrotic regions. Scoring for p-STAT3-Y705 and p-STAT3-S727 was assigned based on both staining proportion and intensity as previously described[5]. For expression intensity of p-Akt, p-ERK and cyclin D1, the integrated absorbance and the area in a photograph were measured using Image-Pro Plus v6.0 software (Media Cybernetics, Inc.). A uniform setting of color segmentation was loaded for counting the integrated absorbance of all the pictures, and the mean p-Akt, p-ERK or cyclin D1 density was calculated as the product of the integrated absorbance/total area.

Detection and quantitation of apoptosis

The terminal deoxynucleotidyl transferase-mediated dUTP nick end labeling (TUNEL) method was based on the specific binding of terminal deoxynucleotidyl transferase to the 3'-OH ends of DNA, ensuring the synthesis of a polydeoxynucleotide polymer. For this purpose, the In Situ Cell Death Detection kit-Peroxidase (Roche) was used according to the manufacturer's directions.

Capture of the photographs and measurement of positive staining density were performed as described previously[11,22]. Briefly, the tissue sections were viewed at × 200 magnification and images were captured. The Apoptosis Index was determined by counting at least 1000 cells in 5 randomly selected fields,using Image-Pro Plus v6.0

Table 1 Sorafenib suppresses tumor growth and metastasis *in vivo* n (%)

Groups (n = 10)	Tumor volume (mm³)	Lung metastasis	Lymph node metastasis	Peritoneal seeding	Ascites
Vehicle	12795.71 ± 2980.56	9/10 (90)	7/10 (70)	3/10 (30)	4/10 (40)
Sorafenib (early)	351.26 ± 97.58[a]	0/10 (0)[b]	0/10 (0)[b]	0/10 (0)[c]	0/10 (0)[c]
Sorafenib (late)	2248.33 ± 971.68[a]	4/10 (40)[b]	0/10 (0)[b]	0/10 (0)[c]	0/10 (0)[c]

[a]$P < 0.001$, Student *t* test (*vs* vehicle group); [b]$P < 0.05$, Fisher's exact test (*vs* vehicle group); [c]$P < 0.05$, Fisher's exact test (*vs* vehicle group).

software (Media Cybernetics, Silver Spring, MD).

Statistical analysis

Statistical analysis was performed with SPSS 16.0 software (SPSS, Chicago, IL). Measurement values were expressed as mean ± SD. The Student *t*-test and Fisher's exact test were used as appropriate. Two-tailed $P < 0.05$ were considered significant.

RESULTS

Sorafenib inhibits tumor growth in vitro

To determine the growth inhibition effect of sorafenib in HCC, HCC cell lines HCCLM3, HepG2 and MH were incubated for 24, 48 and 72 h with sorafenib (0.01-20 μmol/L). As shown in Figure 1A, sorafenib inhibited tumor cell growth in both a time- and dose- dependent manner.

Sorafenib inhibits STAT3 phosphorylation independent of JAK2

Given that STAT3 is constitutively activated in HCC, we next evaluated whether sorafenib could induce HCC growth arrest by inhibiting STAT3. We found that sorafenib inhibited phosphorylation of STAT3 at both Y705 and S727 in a dose-dependent manner. Furthermore, inhibition was evident as early as 2 h after treatment and lasted for 24 h (Figure 1B and 1C) in all HCC cell lines, which corresponded with sorafenib-induced growth inhibition as assessed by MTT assay.

JAK2 is considered as one of the most common activators of STAT3. We therefore determined the effects of sorafenib on JAK2. Western blot analysis showed that JAK2 phosphorylation was not reduced during the 24-h sorafenib treatment (Figure 1B and 1C). In addition, total STAT3 protein and mRNA expression levels also remained unchanged during the 24-h treatment ($P > 0.05$ for all; Figure 1C and 1D).

Sorafenib-induced S727 dephosphorylation is dependent on MEK/ERK

Because 24 h treatment with 10 μmol/L sorafenib significantly inhibited S727 and ERK phosphorylation in HCC lines, we evaluated the effect of the selective MEK inhibitor U0126 in HepG2 and MH cells to determine whether MEK was involved in this effect (Figure 2A). Dephosphorylation of S727, not Y705, was associated with attenuated ERK phosphorylation by U0126, suggesting that sorafenib induced S727 dephosphorylation (but not Y705), at least partly, through inhibiting MEK/

ERK phosphorylation.

Sorafenib-induced Y705 dephosphorylation is dependent on PI3K/Akt

A 2-h treatment with the PI3K inhibitor, LY294002, significantly inhibited phosphorylation of Y705, but not S727, in a dose-dependent manner (Figure 2B). This inhibitory effect lasted for 24 h after treatment (Figure 2B), which was in parallel with results of sorafenib treatment. Similarly, we found that knockdown of Akt expression and activation by siRNA also significantly inhibited phosphorylation of Y705, but not S727, in HepG2 and MH cell lines (Figure 2C), suggesting that the PI3K/Akt may be responsible for Y705 phosphorylation in HCC. We further found that sorafenib could inhibit Akt activation in HCC cell lines, mainly at lower concentrations (Figure 2D). Collectively, these results suggested that sorafenib could downregulate Y705 phosphorylation in part by blocking the PI3K/Akt pathway.

Apart from PI3K/Akt, some other effectors, such as SHP2[23], may also take an active part in Y705 dephosphorylation. Here, we also determined the effects of sorafenib on SHP2. Western blot analysis showed that SHP2 phosphorylation was not affected during the 24 h sorafenib treatment (Figure 2E). Cyclin D1 is an important target gene of STAT3. Our data also showed that the expression of cyclin D1 decreased in HCC cells treated with sorafenib (Figure 2E).

Sorafenib inhibits HCC tumor growth and metastasis in vivo

Various manifestations exhibited by our immunocompetent rat model of HCC including local growth, regional invasion, spontaneous metastasis to lungs, lymph nodes, and peritoneal seeding (Figure 3A), as well as molecular signatures like constitutively active JAK2, SHP2, STAT3, Akt and ERK, are similar to those observed in HCC patients.

As shown in Table 1, sorafenib significantly reduced tumor volume (mean tumor volume: vehicle control group, 12795.71 ± 2980.56 mm³; sorafenib late treatment group, 2248.33 ± 971.68 mm³; $P < 0.001$). Furthermore, the primary tumor volume was even lower in the sorafenib early treatment group (mean tumor volume: 351.26 ± 97.58 mm³; $P < 0.001$). Sorafenib treatment (early and late) also suppressed lung and lymph node metastasis compared with the vehicle control ($P < 0.05$; Figure 3A and 3B). Sorafenib treatment reduced peritoneal seeding and bloody ascites, but these differences
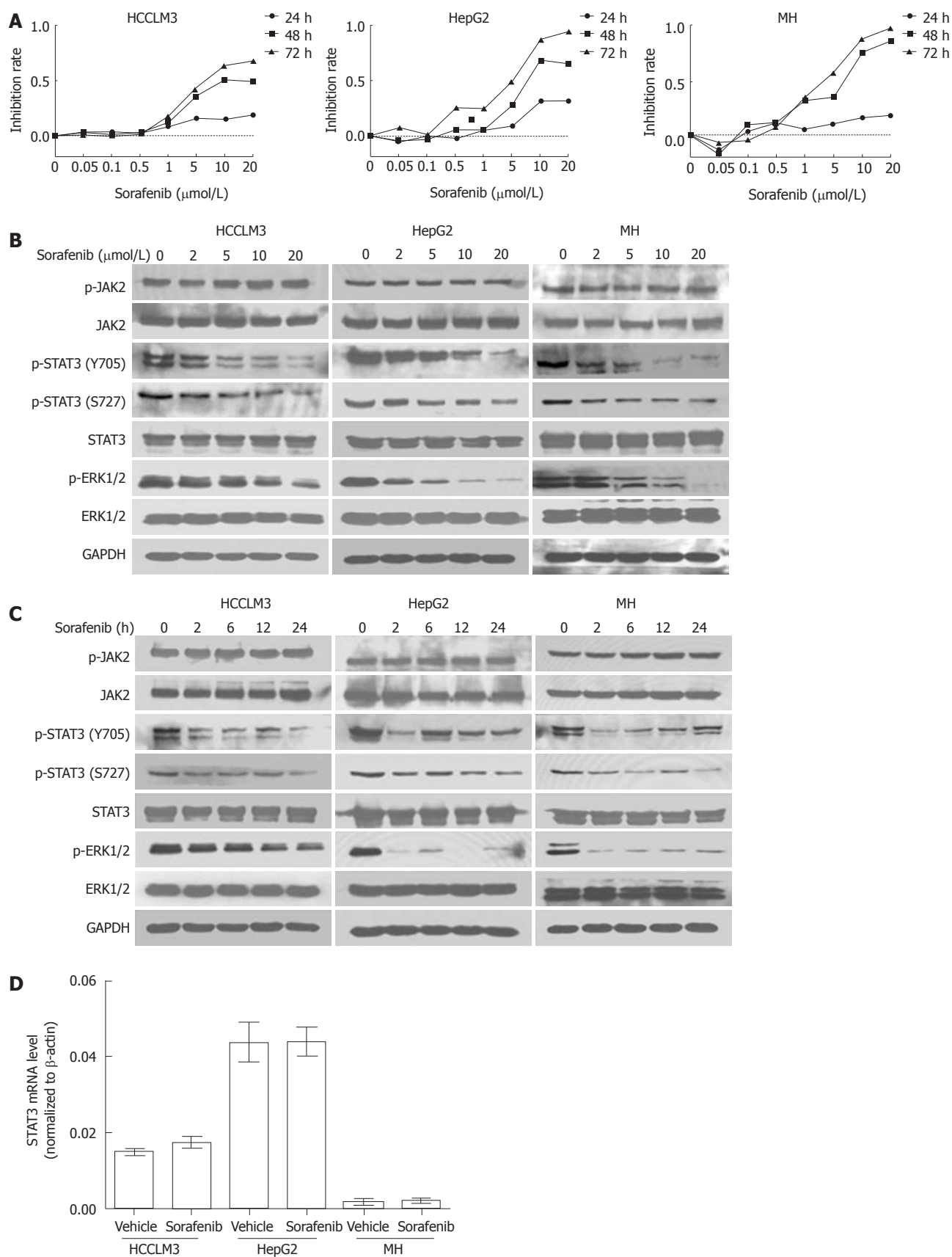
Figure 1 Inhibition of signal transducer and activator of transcription 3 signaling by sorafenib is associated with reduced cell proliferation. A: Sorafenib inhibited cell proliferation in a time and dose-dependent manner, as assessed by the MTT assay; B: Sorafenib inhibited phosphorylation of signal transducer and activator of transcription 3 (STAT3) and extracellular signal-regulated kinase 1/2, but not janus kinase 2 (JAK2), in a dose-dependent manner. Hepatocellular carcinoma (HCC) cells were exposed to sorafenib for 2 h, and proteins were analyzed by Western blot; C: Sorafenib durably inhibited phosphorylation of STAT3 and ERK1/2 but not JAK2. HCC cells were treated with 10 μmol/L sorafenib for different durations, and cell lysates were analyzed by Western blotting; D: Sorafenib did not affect STAT3 mRNA levels in HCC cell lines ($P > 0.05$ for all). After 24-h sorafenib treatment (10 μmol/L), STAT3 mRNA levels were analyzed by qRT-PCR.
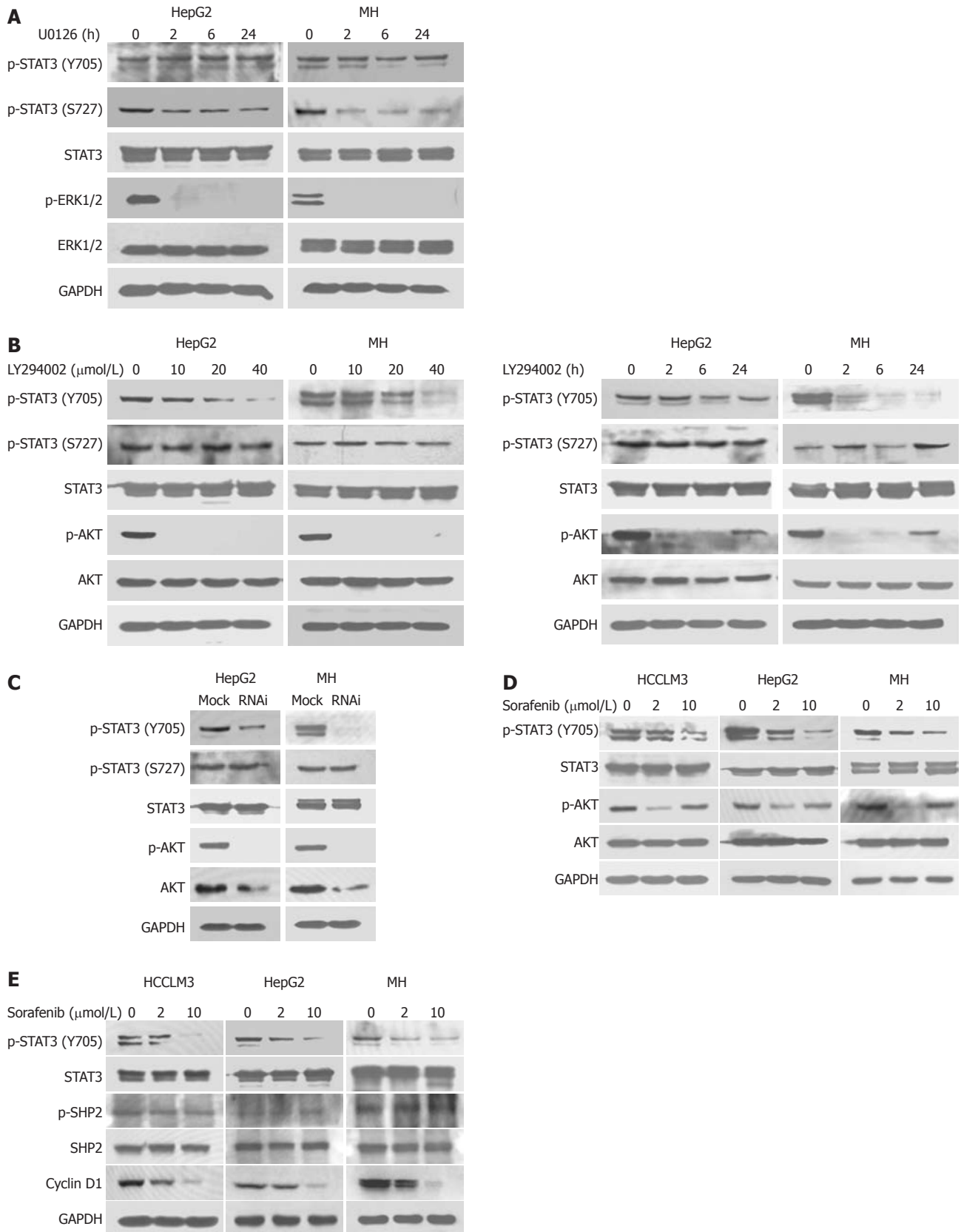
Figure 2 Inhibition of signal transducer and activator of transcription 3 signaling in hepatocellular carcinoma. A: U0126 (20 μmol/L) durably inhibited phosphorylation of signal transducer and activator of transcription 3 (STAT3) (S727) in HepG2 and Morris hepatoma (MH) cell lines; B: A 2-h exposure to LY294002 inhibited phosphorylation of STAT3 (Y705) in HepG2 and MH cells in a dose-dependent manner (left). LY294002 (20 μmol/L) durably inhibited phosphorylation of STAT3 (Y705) in HepG2 and MH cells (right); C: Akt silencing by siRNA inhibited phosphorylation of STAT3 (Y705, but not S727) in HepG2 and MH cells; D: A 2-h exposure to sorafenib inhibited phosphorylation of Akt, mainly at low concentration (2 μmol/L) in HCCLM3, HepG2, and MH cells; E: Sorafenib promoted Y705 dephosphorylation and obviously reduced the expression levels of cyclin D1 regardless of shatterproof 2 (SHP2).
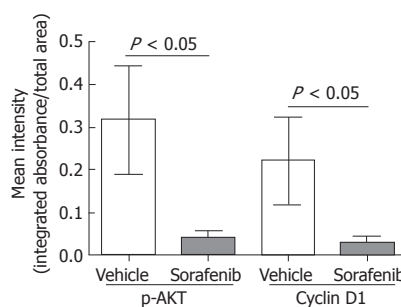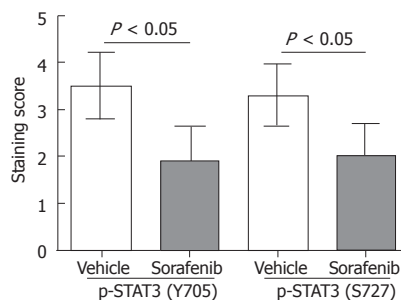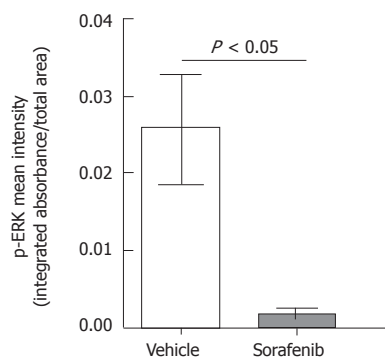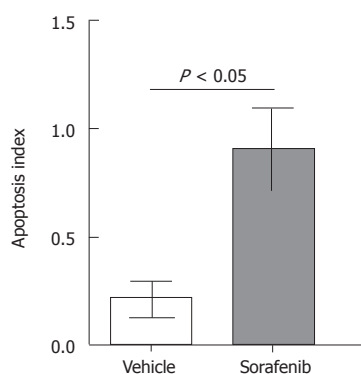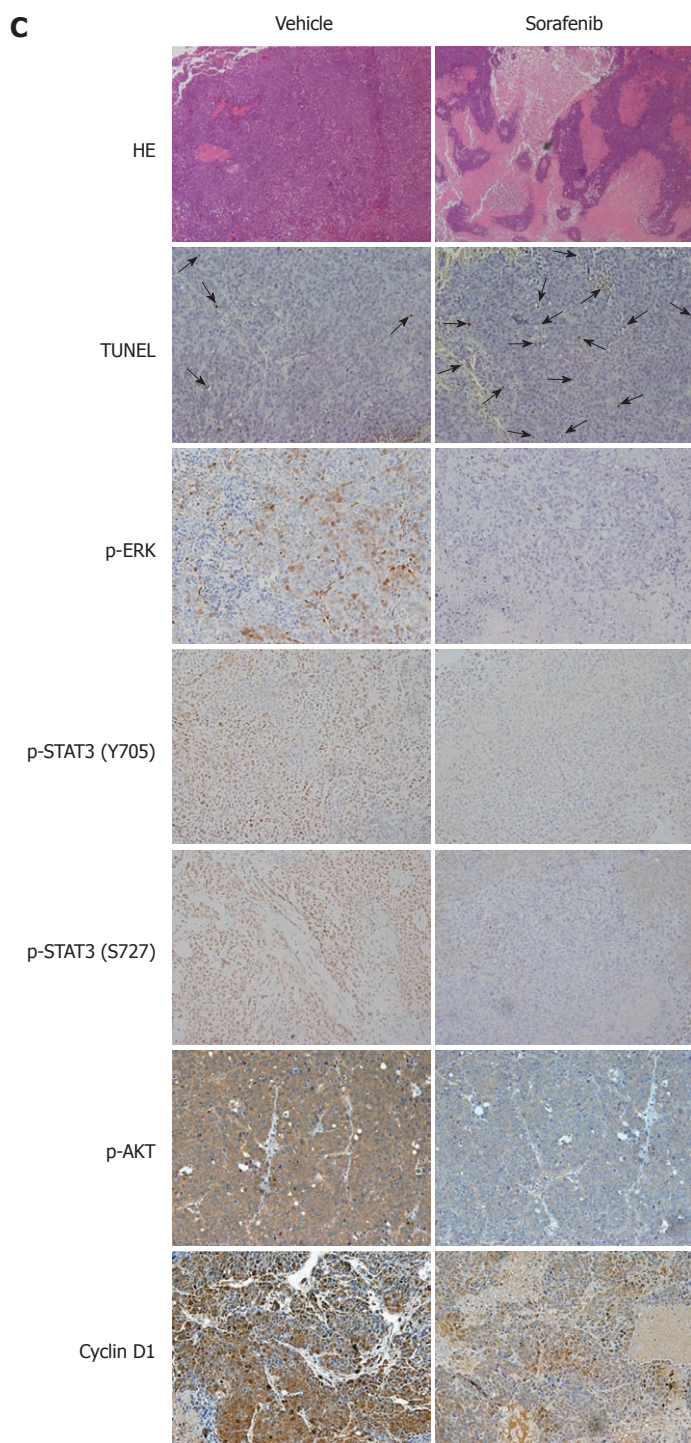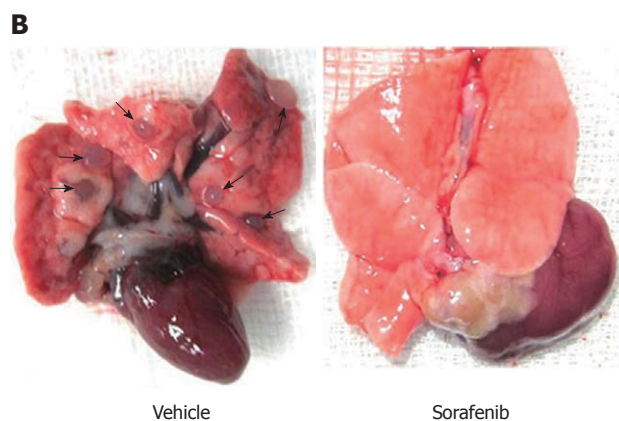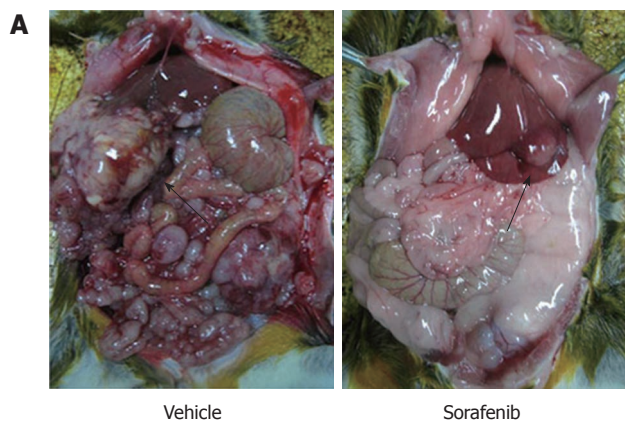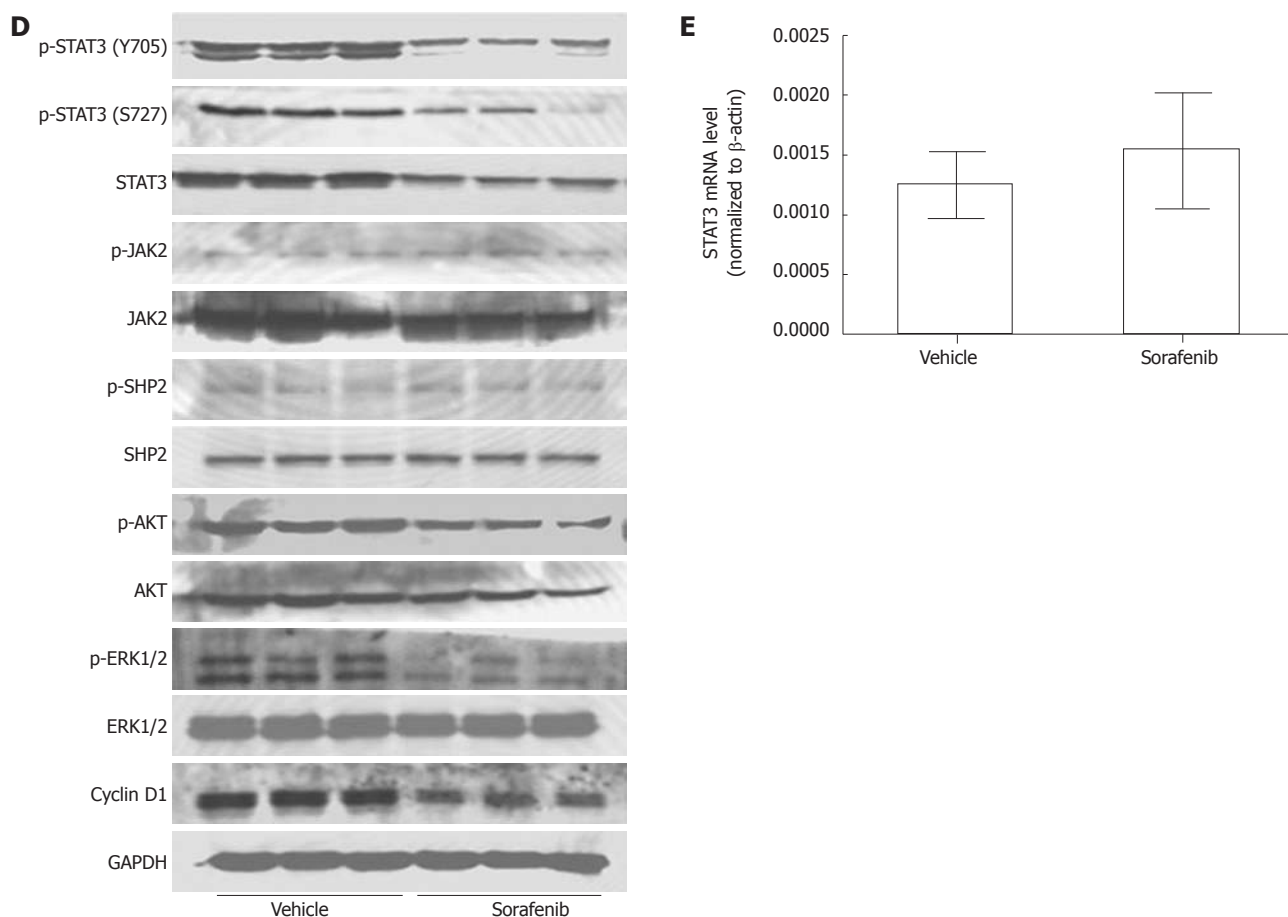
Figure 3 Inhibition of tumor growth and metastasis by sorafenib *in vivo*. Rats with morris hepatoma (MH) tumors were treated with vehicle or sorafenib (30 mg/kg per day) starting on day 17 after tumor implantation. Tumors were removed on day 38 following implantation; A: Tumor growth and abdominal lymph node metastasis were reduced by sorafenib treatment (arrows); B: Sorafenib treatment reduced lung metastasis (arrows); C: Significant tumor necrosis in the sorafenib-treated group was visualized by hematoxylin-eosin staining (magnification, × 40). As shown by TUNEL (arrows), sorafenib also induced tumor cell apoptosis significantly (apoptosis index, 0.217 ± 0.825 *vs* 0.909 ± 0.189; *P* < 0.05; magnification, × 200). Immunohistochemical analysis showed that the expression levels of cyclin D1 and phosphorylation of signal transducer and activator of transcription 3 (STAT3) (Y705 and S727), Akt, and extracellular signal-regulated kinase (ERK) were significantly reduced by sorafenib treatment (*P* < 0.05 for all; magnification, × 200); D: Sorafenib reduced phosphorylation of STAT3, Akt, and ERK, but not Janus kinase 2 and shatterproof 2. Sorafenib also reduced the expression levels of cyclin D1 significantly; E: Sorafenib did not affect STAT3 mRNA levels in rat tumor tissues (*P* > 0.05).

were not significant (*P* > 0.05). Obvious weight loss or death (data not shown) was not observed in sorafenib-treated rats, suggesting that sorafenib was well tolerated and effective in this rat HCC model.

Significant tumor necrosis in the sorafenib treatment group was visualized by hematoxylin-eosin staining (Figure 3C). As shown by TUNEL, sorafenib also induced tumor cell apoptosis significantly (apoptosis index, 0.217 ± 0.825 *vs* 0.909 ± 0.189; *P* < 0.05; Figure 3C). Immunohistochemistry confirmed that phosphorylation of STAT3 (Y705 and S727), Akt and ERK was much lower in the sorafenib treatment group than in the vehicle control (*P* < 0.05 for all; Figure 3C). Western blot analysis also indicated that the dose of sorafenib used in this study was sufficient to inhibit phosphorylation of Akt, ERK and STAT3 in tumors (Figure 3D), which was consistent with its antitumor effects. As with *in vitro* results, sorafenib *in vivo* treatment did not reduce the STAT3 mRNA level (*P* > 0.05; Figure 3E), nor JAK2 and SHP2 phosphorylation (Figure 3D). In addition, expression of STAT3-related cyclin D1 was reduced in the sorafenib

late treatment group (*P* < 0.05; Figure 3C and 3D).

DISCUSSION

STAT3 is constitutively active in most tumor cells and not in normal cells, and hence represents an attractive molecular target[24]. Here, we showed that sorafenib inhibited STAT3 phosphorylation: (1) at S727 through the MEK/ERK signaling pathway; (2) at Y705 by blocking PI3K/Akt signaling pathways; and (3) independent of JAK and SHP2, thereby inhibiting HCC tumor growth *in vitro* and *in vivo*. Although some studies have reported that sorafenib inhibits STAT3 signaling in some cancers including HCC[12-16], to the best of our knowledge, this is the first report demonstrating the full inhibition of STAT3 activity on 2 phosphorylating residues by sorafenib acting on distinct underlying mechanisms in HCC (Figure 4).

Phosphorylation of STAT3 at Y705 enables its dimerization, nuclear translocation, DNA binding, and gene transcription[25], whereas phosphorylation of an-
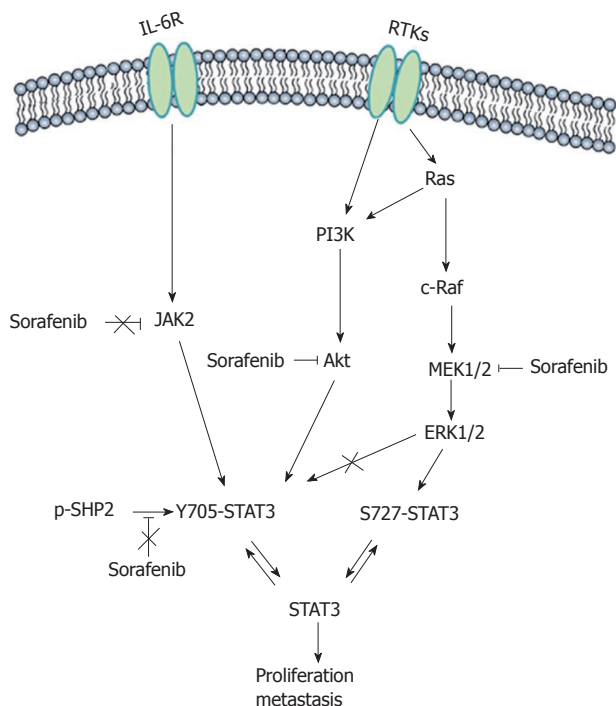
Figure 4 Signaling pathways involved in sorafenib-induced inhibition of signal transducer and activator of transcription 3 phosphorylation. In hepatocellular carcinoma, extracellular signal-regulated kinase-related pathways regulate signal transducer and activator of transcription 3 (STAT3) phosphorylation at S727, and phosphatidylinositol-3-kinase (PI3K)/Akt can be responsible for phosphorylation at Y705. Thus, sorafenib inhibits STAT3 phosphorylation in part through blockade of the mitogen-activated protein kinase kinase (MEK)/extracellular signal-regulated kinase (ERK)/STAT3 and PI3K/Akt/STAT3 signaling pathways, regardless of the Janus kinase 2 and phosphatase shatterproof 2.

other conserved STAT3 residue, S727, enhances STAT3 transcriptional activity[26]. Cooperation of tyrosine and serine phosphorylation is necessary for the full activation of STAT3[27]. We found that STAT3 was constitutively phosphorylated at Y705 and S727 in HCC and sorafenib inhibited phosphorylation of the both sites among HCC cells that exhibited different molecular or genetic characteristics. The inhibition was evident as early as 2 h after treatment and lasted for 24 h, suggesting the actions of sorafenib are relatively rapid and prolonged. Furthermore, we identified the potential mechanisms involved in blocking STAT3 signaling.

First, we observed that sorafenib induced STAT3 dephosphorylation at S727 was accompanied by simultaneously blocked MEK/ERK signaling. Similar results were observed with the MEK inhibitor U0126, indicating that ERK-related pathways participate in the regulation of STAT3 in HCC. We reasoned that sorafenib-induced S727 dephosphorylation may be mediated through the MEK/ERK/STAT3 pathway. However, the phosphorylation of both S727 and Y705 were inhibited by sorafenib, whereas U0126 produced no obvious effects on Y705. Therefore, yet unidentified signaling pathways may be involved in sorafenib-induced Y705 dephosphorylation of STAT3.

To clarify this point, we exposed HCC cells to both

the PI3K inhibitor LY294002 and Akt knockdown, and found these treatments resulted in Y705 dephosphorylation. We thus inferred that PI3K/Akt pathway was involved in Y705 dephosphorylation in HCC. Furthermore, we found sorafenib could also inhibit Akt phosphorylation, suggesting that sorafenib could downregulate Y705 phosphorylation in part by blocking the PI3K/Akt pathway. Given that the PI3K/Akt pathway is an important downstream effector of RTKs[10], and that RTKs are the major well established targets of sorafenib, we propose that RTK inhibition by sorafenib may be responsible for Akt dephosphorylation in HCC. However, to some extent, Akt dephosphorylation was not correlated well with the inhibition of Y705 phosphorylation by sorafenib. Some other mechanisms, besides PI3K/Akt, may also be involved in Y705 dephosphorylation by sorafenib that need further investigation.

In addition, as a first attempt to elucidate the STAT3 signaling pathways involved in sorafenib-treated HCC cells, we examined the effect of sorafenib on JAK2 and SHP2 activation. JAK2 is a typical non-RTK involved in interleukin-6 intracellular signaling that activates STAT3[28]. SHP2, a cytoplasmic tyrosine phosphatase, has been recently shown to operate in sorafenib induced STAT3 dephosphorylation in cholangiocarcinoma[29]. However, both sorafenib-treated and untreated HCC cells contained constitutively activated JAK2 and SHP2, indicating that sorafenib promoted STAT3 dephosphorylation regardless of JAK2 and SHP2. Meanwhile, we did not find that total STAT3 protein expression and mRNA levels were affected.

Because host immune responses play a critical role in hepatocarcinogenesis, invasion and dissemination[30,31], we chose an immunocompetent model for our *in vivo* studies. In this model, sorafenib increased tumor necrosis, induced tumor cell apoptosis and decreased tumor growth, as compared with control treatment. Importantly, consistent with *in vitro* results, *in vivo* sorafenib treatment significantly inhibited STAT3 activity at both Y705 and S727 with concomitant dephosphorylation of Akt and ERK, while dephosphorylation of JAK2 and SHP2 was not observed. In addition, the expression levels of cyclin D1, an important target gene of STAT3, were also reduced accordant with STAT3 inhibition both *in vitro* and *in vivo*.

In conclusion, we demonstrated that sorafenib is capable of inhibiting HCC growth and metastasis by suppressing STAT3 activity. PI3K/Akt and MEK/ERK signaling pathways may be collectively involved in inhibiting STAT3 activity, independent of SHP2 and JAK2. Our findings not only elucidate an additional potential molecular target of sorafenib, but also provide a rational basis for the development of combination strategies to maximize the HCC response.

COMMENTS

Background

Recent studies have shown that signal transducer and activator of transcription 3 (STAT3) is constitutively activated in hepatocellular carcinoma (HCC) and

may be an attractive molecular target. Sorafenib is a multikinase inhibitor that has shown efficacy against advanced HCC. This study investigated the molecular mechanisms of STAT3 inhibition by sorafenib in HCC.

Research frontiers

STAT3 plays a critical role in transcriptional regulation of genes that are involved in tumor cell proliferation, survival and invasion, thus targeting of STAT3 activation may prove to be an effective approach to controlling HCC. Recently, sorafenib has been shown to suppress tumor growth by decreasing STAT3 phosphorylation in a group of human malignancies including HCC. However, thus far, the exact molecular mechanisms by which sorafenib inhibited STAT3 were not fully elucidated.

Innovations and breakthroughs

Although some studies have reported that sorefenib inhibits STAT3 signaling in some cancers including HCC, to the best of our knowledge, this is the first report demonstrating that sorafenib inhibits growth and metastasis of HCC by the full inhibition of STAT3 activity on 2 phosphorylating residues involved in the distinct underlying mechanism of HCC.

Applications

The findings not only elucidate an additional potential molecular target of sorafenib, but also provide a rational basis for the development of combination strategies to maximize the HCC response.

Terminology

STAT3, an important transcription factor, plays a critical role in transcriptional regulation of genes that are involved in tumor cell proliferation, survival and invasion. STAT3 is constitutively activated in diverse cancer cell types and has been shown to be an essential signaling molecule in tumorigenesis through its transcriptional activity on tumor-associated genes.

Peer review

In this manuscript, the authors showed the mechanisms of the suppression of HCC growth by sorafenib *in vivo* and *in vitro*. The study is organized well, the results are interesting and the manuscript is written properly.

REFERENCES

1   **El-Serag HB**, Rudolph KL. Hepatocellular carcinoma: epidemiology and molecular carcinogenesis. *Gastroenterology* 2007; **132**: 2557-2576

2   **Abou-Alfa GK**. Hepatocellular carcinoma: molecular biology and therapy. *Semin Oncol* 2006; **33**: S79-S83

3   **Darnell JE**. Transcription factors as targets for cancer therapy. *Nat Rev Cancer* 2002; **2**: 740-749

4   **Yu H**, Pardoll D, Jove R. STATs in cancer inflammation and immunity: a leading role for STAT3. *Nat Rev Cancer* 2009; **9**: 798-809

5   **Yang SF**, Wang SN, Wu CF, Yeh YT, Chai CY, Chunag SC, Sheen MC, Lee KT. Altered p-STAT3 (tyr705) expression is associated with histological grading and intratumour microvessel density in hepatocellular carcinoma. *J Clin Pathol* 2007; **60**: 642-648

6   **Aggarwal BB**, Sethi G, Ahn KS, Sandur SK, Pandey MK, Kunnumakkara AB, Sung B, Ichikawa H. Targeting signal-transducer-and-activator-of-transcription-3 for prevention and therapy of cancer: modern target but ancient solution. *Ann N Y Acad Sci* 2006; **1091**: 151-169

7   **Masuda M**, Wakasaki T, Suzui M, Toh S, Joe AK, Weinstein IB. Stat3 orchestrates tumor development and progression: the Achilles' heel of head and neck cancers? *Curr Cancer Drug Targets* 2010; **10**: 117-126

8   **Yu H**, Jove R. The STATs of cancer--new molecular targets come of age. *Nat Rev Cancer* 2004; **4**: 97-105

9   **Li WC**, Ye SL, Sun RX, Liu YK, Tang ZY, Kim Y, Karras JG, Zhang H. Inhibition of growth and metastasis of human hepatocellular carcinoma by antisense oligonucleotide targeting signal transducer and activator of transcription 3. *Clin Cancer Res* 2006; **12**: 7140-7148

10   **Wilhelm SM**, Carter C, Tang L, Wilkie D, McNabola A, Rong H, Chen C, Zhang X, Vincent P, McHugh M, Cao Y, Shujath J, Gawlak S, Eveleigh D, Rowley B, Liu L, Adnane L, Lynch M, Auclair D, Taylor I, Gedrich R, Voznesensky

A, Riedl B, Post LE, Bollag G, Trail PA. BAY 43-9006 exhibits broad spectrum oral antitumor activity and targets the RAF/MEK/ERK pathway and receptor tyrosine kinases involved in tumor progression and angiogenesis. *Cancer Res* 2004; **64**: 7099-7109

11   **Liu L**, Cao Y, Chen C, Zhang X, McNabola A, Wilkie D, Wilhelm S, Lynch M, Carter C. Sorafenib blocks the RAF/MEK/ERK pathway, inhibits tumor angiogenesis, and induces tumor cell apoptosis in hepatocellular carcinoma model PLC/PRF/5. *Cancer Res* 2006; **66**: 11851-11858

12   **Yang F**, Van Meter TE, Buettner R, Hedvat M, Liang W, Kowolik CM, Mepani N, Mirosevich J, Nam S, Chen MY, Tye G, Kirschbaum M, Jove R. Sorafenib inhibits signal transducer and activator of transcription 3 signaling associated with growth arrest and apoptosis of medulloblastomas. *Mol Cancer Ther* 2008; **7**: 3519-3526

13   **Yang F**, Brown C, Buettner R, Hedvat M, Starr R, Scuto A, Schroeder A, Jensen M, Jove R. Sorafenib induces growth arrest and apoptosis of human glioblastoma cells through the dephosphorylation of signal transducers and activators of transcription 3. *Mol Cancer Ther* 2010; **9**: 953-962

14   **Huang S**, Sinicrope FA. Sorafenib inhibits STAT3 activation to enhance TRAIL-mediated apoptosis in human pancreatic cancer cells. *Mol Cancer Ther* 2010; **9**: 742-750

15   **Zhao W**, Zhang T, Qu B, Wu X, Zhu X, Meng F, Gu Y, Shu Y, Shen Y, Sun Y, Xu Q. Sorafenib induces apoptosis in HL60 cells by inhibiting Src kinase-mediated STAT3 phosphorylation. *Anticancer Drugs* 2011; **22**: 79-88

16   **Chen KF**, Tai WT, Liu TH, Huang HP, Lin YC, Shiau CW, Li PK, Chen PJ, Cheng AL. Sorafenib overcomes TRAIL resistance of hepatocellular carcinoma cells through the inhibition of STAT3. *Clin Cancer Res* 2010; **16**: 5189-5199

17   **Ye QH**, Qin LX, Forgues M, He P, Kim JW, Peng AC, Simon R, Li Y, Robles AI, Chen Y, Ma ZC, Wu ZQ, Ye SL, Liu YK, Tang ZY, Wang XW. Predicting hepatitis B virus-positive metastatic hepatocellular carcinomas using gene expression profiling and supervised machine learning. *Nat Med* 2003; **9**: 416-423

18   **Li Y**, Tang Y, Ye L, Liu B, Liu K, Chen J, Xue Q. Establishment of a hepatocellular carcinoma cell line with unique metastatic characteristics through in vivo selection and screening for metastasis-related genes through cDNA microarray. *J Cancer Res Clin Oncol* 2003; **129**: 43-51

19   **Piguet AC**, Semela D, Keogh A, Wilkens L, Stroka D, Stoupis C, St-Pierre MV, Dufour JF. Inhibition of mTOR in combination with doxorubicin in an experimental model of hepatocellular carcinoma. *J Hepatol* 2008; **49**: 78-87

20   **Gao Q**, Wang XY, Qiu SJ, Yamato I, Sho M, Nakajima Y, Zhou J, Li BZ, Shi YH, Xiao YS, Xu Y, Fan J. Overexpression of PD-L1 significantly associates with tumor aggressiveness and postoperative recurrence in human hepatocellular carcinoma. *Clin Cancer Res* 2009; **15**: 971-979

21   **Yang R**, Rescorla FJ, Reilly CR, Faught PR, Sanghvi NT, Lumeng L, Franklin TD, Grosfeld JL. A reproducible rat liver cancer model for experimental therapy: introducing a technique of intrahepatic tumor implantation. *J Surg Res* 1992; **52**: 193-198

22   **Wang Z**, Zhou J, Fan J, Qiu SJ, Yu Y, Huang XW, Tang ZY. Effect of rapamycin alone and in combination with sorafenib in an orthotopic model of human hepatocellular carcinoma. *Clin Cancer Res* 2008; **14**: 5124-5130

23   **Zheng H**, Alter S, Qu CK. SHP-2 tyrosine phosphatase in human diseases. *Int J Clin Exp Med* 2009; **2**: 17-25

24   **Barré B**, Vigneron A, Perkins N, Roninson IB, Gamelin E, Coqueret O. The STAT3 oncogene as a predictive marker of drug resistance. *Trends Mol Med* 2007; **13**: 4-11

25   **Aggarwal BB**, Kunnumakkara AB, Harikumar KB, Gupta SR, Tharakan ST, Koca C, Dey S, Sung B. Signal transducer and activator of transcription-3, inflammation, and cancer: how intimate is the relationship? *Ann N Y Acad Sci* 2009;

1171: 59-76

26   **Lufei C**, Koh TH, Uchida T, Cao X. Pin1 is required for the Ser727 phosphorylation-dependent Stat3 activity. *Oncogene* 2007; **26**: 7656-7664

27   **Aziz MH**, Manoharan HT, Church DR, Dreckschmidt NE, Zhong W, Oberley TD, Wilding G, Verma AK. Protein kinase Cepsilon interacts with signal transducers and activators of transcription 3 (Stat3), phosphorylates Stat3Ser727, and regulates its constitutive activation in prostate cancer. *Cancer Res* 2007; **67**: 8828-8838

28   **Colomiere M**, Ward AC, Riley C, Trenerry MK, Cameron-Smith D, Findlay J, Ackland L, Ahmed N. Cross talk of signals between EGFR and IL-6R through JAK2/STAT3 mediate epithelial-mesenchymal transition in ovarian carcinomas. *Br J Cancer* 2009; **100**: 134-144

29   **Blechacz BR**, Smoot RL, Bronk SF, Werneburg NW, Sirica AE, Gores GJ. Sorafenib inhibits signal transducer and activator of transcription-3 signaling in cholangiocarcinoma cells by activating the phosphatase shatterproof 2. *Hepatology* 2009; **50**: 1861-1870

30   **Budhu A**, Forgues M, Ye QH, Jia HL, He P, Zanetti KA, Kammula US, Chen Y, Qin LX, Tang ZY, Wang XW. Prediction of venous metastases, recurrence, and prognosis in hepatocellular carcinoma based on a unique immune response signature of the liver microenvironment. *Cancer Cell* 2006; **10**: 99-111

31   **Gao Q**, Qiu SJ, Fan J, Zhou J, Wang XY, Xiao YS, Xu Y, Li YW, Tang ZY. Intratumoral balance of regulatory and cytotoxic T cells is associated with prognosis of hepatocellular carcinoma after resection. *J Clin Oncol* 2007; **25**: 2586-2593

S- Editor Tian L   **L- Editor** Cant MR   **E- Editor** Li JY